Adaptive time-dependent density-matrix renormalization-group technique for calculating the conductance of strongly correlated nanostructures

K. A. Al-Hassanieh,[1,2] A. E. Feiguin,[3] J. A. Riera,[4] C. A. Büsser,[1] and E. Dagotto[1]
[1]*Condensed Matter Sciences Division, Oak Ridge National Laboratory, Oak Ridge, Tennessee 37831, USA and Department of Physics, The University of Tennessee, Knoxville, Tennessee 37996, USA*
[2]*National High Magnetic Field Laboratory and Department of Physics, Florida State University, Tallahassee, Florida 32306, USA*
[3]*Microsoft Project Q, The University of California at Santa Barbara, Santa Barbara, California 93106, USA*
[4]*Universidad Nacional de Rosario, Avenida Pellegrini 250, 2000-Rosario, Argentina*
(Received 17 January 2006; published 3 May 2006)

A procedure based on the recently developed "adaptive" time-dependent density-matrix-renormalization-group (DMRG) technique is presented to calculate the zero temperature conductance of nanostructures, such as quantum dots (QDs) or molecular conductors, when represented by a small number of active levels. The leads are modeled using noninteracting tight-binding Hamiltonians. The ground state at time zero is calculated at zero bias. Then, a small bias is applied between the two leads, the wave function is DMRG evolved in time, and currents are measured as a function of time. Typically, the current is expected to present periodicities over long times, involving intermediate well-defined plateaus that resemble steady states. The conductance can be obtained from those steady-state-like currents. To test this approach, several cases of interacting and noninteracting systems have been studied. Our results show excellent agreement with exact results in the noninteracting case. More importantly, the technique also reproduces quantitatively well-established results for the conductance and local density of states in both the cases of one and two coupled interacting QDs. The technique also works at finite bias voltages, and it can be extended to include interactions in the leads.

DOI: 10.1103/PhysRevB.73.195304 PACS number(s): 73.63.−b, 71.27.+a, 72.10.−d, 85.65.+h

I. INTRODUCTION

The rapidly developing investigations in the area of nanometer-scale systems and its concomitant potential technological applications in real devices have induced considerable interest in the study of electrical transport through small molecules and quantum dots. In fact, the construction of molecular electronic devices[1,2] is among the most exciting areas of investigation in physics, and theoretical guidance is needed for the success of this vast effort. Molecules can change their shape and position relative to the leads as electrons enter or leave the molecule, making the study of these systems very challenging. Moreover, Coulomb correlations cannot be neglected in small devices. For a conceptual understanding of these complex systems, it is imperative to develop models and unbiased many-body methods that rely on a minimal number of assumptions in order to accurately handle both strong Coulombic and electron-phonon couplings. Quantum dots (QDs) constructed using conventional semiconductor technology also provide an important playground for the analysis of transport properties in nanoscopic systems, and the theoretical challenges in this context are equally important.[3]

The conductance of small nanoscopic systems can be theoretically estimated using a variety of techniques. Among the most popular approaches are the *ab initio* calculations using density functional theory (DFT). These one-electron self-consistent methods have been successful in describing various I-V characteristics.[4–6] However, the applicability of these ideas must be carefully scrutinized, as recently remarked by Muralidharan *et al.*[7] For example, it is clear that in small molecules charging effects are important, and they effectively act as quantum dots in the Coulomb blockade regime. Moreover, techniques that do not take into account the strong correlation between electrons cannot capture important effects, such as the Kondo resonance (arising from the coupling between localized spins and conduction electrons), which induces a new channel for transport in a variety of small systems.[8,9] In addition, it is well known that several bulk materials, such as transition metal oxides, cannot be described with *ab initio* methods that neglect correlations. The complexity of their behavior, including potentially useful effects such as large magnetoresistances in Mn oxides,[10] may manifest in nanoscopic systems as well, and the use of strongly correlated materials in nanodevices may lead to interesting applications. To study all these systems (small molecules, quantum dots, and, in general, nanodevices that include strongly correlated materials), techniques beyond DFT must be developed.

A similar challenge occurred before in the study of bulk materials and several years of research have shown that the following two-step process leads to profound insights. The first step consists of a simple modeling of the material, typically either deducing the relevant degrees of freedom from atomistic considerations when the states are very localized or borrowing from band structure calculations to isolate the minimal ingredients needed to capture the essence of the problem. The second step, the hardest, is solving the resulting model, which is typically of a tight-binding nature with the addition of Coulombic and phononic couplings. In the strong coupling regime, the use of numerical techniques provides the most reliable unbiased approach for the approximate investigation of tight-binding-like models with Coulombic interactions.[11] As a consequence, a natural path

FIG. 1. (Color online) Schematic representation of the geometry used in our study. The leads are modeled by tight-binding Hamiltonians. The ground state at time zero is calculated at zero bias. Then, a finite bias ΔV is applied between the two leads (without ramping time for simplicity, but this can be changed in future studies) and the resulting current is measured.

toward the study of transport in strongly correlated nanoscopic systems can also start with simple models and use computational techniques for their analysis. It is the main purpose of this paper to propose a technique that can be used to study transport in systems described by strongly correlated electronic models.

The method to calculate conductances proposed here relies on the successful density-matrix-renormalization-group (DMRG) technique.[12,13] Although, in principle, this method is applicable only to quasi-one-dimensional models, such a geometry is quite acceptable in several nanoscopic important problems, including transport in arrays of quantum dots or using small molecules as bridges between leads. However, a straightforward application of the original DMRG methodology is not immediately useful to study transport, particularly when arbitrarily large external electric and magnetic fields, with potentially complicated time dependences, are switched on and off at particular times. Nevertheless, progress toward a computational tool for these type of problems has been steady in recent years. For instance, important numerical methods for dynamical DMRG studies were presented to handle frequency-dependent spectral functions.[14–16] More directly focusing on real-time investigations, interesting techniques were proposed.[17] Although useful for many qualitative applications, these methods are, in general, not as accurate and stable as needed for the detailed study of finite bias transport in complicated nanosystems. The reason is that the method of Ref. 17 is "static" in the sense that the truncated Hilbert space found to be optimal at time $t=0$, namely, before switching on the external fields, is kept at all times. This approach breaks down after relatively short times, since extra states are needed for a proper description of transport at finite times. A further approximation to improve on this first proposal is to enlarge substantially the initial Hilbert space so that it remains suitable for properties calculated at finite times.[18] This technique has the problem that the number of states grows rapidly with the simulation time, and eventually, it becomes impractical. Nevertheless, the method has been successfully used to study the propagation of a density excitation in an interacting clean system.[19]

Recently, important developments have led to the "adaptive" time-dependent version of the DMRG method that is efficient over long times and, thus, it is suitable to handle the problems we are focusing on (for a detailed review, see Ref. 20). The method to be used here was developed independently by White and Feiguin[21] and Daley *et al.*,[22] after the idea of how to do time-evolution to a matrix product was introduced by Vidal,[23] and relies on an adaptive optimal Hilbert space that follows the state as time grows. The method is

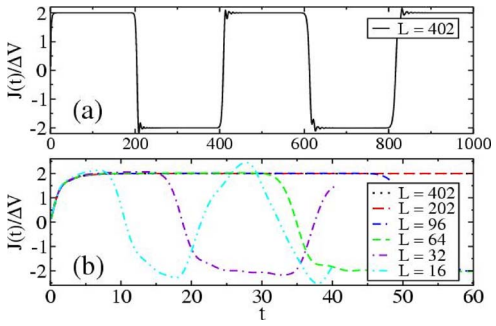

FIG. 2. (Color online) Exact results for $J(t)/\Delta V$ (in units of e^2/h) vs time (in units of $\hbar/t_{\text{leads}}$), for the noninteracting 1QD case obtained with clusters of different lengths (L) and $\Delta V=0.001$. (a) $J(t)/\Delta V$ obtained with a large cluster ($L=402$). $J(t)/\Delta V$ shows clear steady-state plateaus at $\pm 2e^2/h$. The periodic changes in the current direction are caused by its reflection at the open boundaries of the cluster. (b) $J(t)/\Delta V$ obtained with decreasing L. The steady-state plateau is obtained even with $L=32$. The current is quasiperiodic with a period proportional to L. The parameters used are $V_g=U=0$ and $t'=0.4$.

based on a Suzuki-Trotter breakup of the evolution operator, and as a consequence, a Trotter truncation error is introduced. Fortunately, this systematic error can be easily estimated and controlled. The adaptive DMRG numerical method will only be briefly reviewed below since our proposal uses the technique to calculate conductances, but does not modify the method itself. The reader should consult the original literature[21,22] for more details. It is important to remark that the technique is easy to implement once a ground-state DMRG code is prepared and, moreover, the time-evolution is stable, as shown explicitly in our results and in some previous investigations (further improvements can be added with the time-step targeting method recently proposed by Feiguin and White[25]). The conclusion of our effort documented below is that the adaptive method provides accurate results for the calculation of conductances. The technique has passed the test of noninteracting electrons as well as the cases of one and two interacting quantum dots, where a subtle Kondo effect occurs. Moreover, the method is not restricted to small biases, but it produces reasonable answers at finite bias as well. As a consequence, it has the potential of being the method of choice to study transport under both weak and strong external fields, in small nanostructures of substantial complexity. Multilevel model Hamiltonians, possibly inspired by *ab initio* calculations, can be used to describe the "bridge" between leads. In addition, the method is particularly transparent since it relies on the straightforward calculation of a current in the presence of a voltage, rather than relying on other indirect linear-response formulas.

Of course, the reader must be aware that the method is not of unlimited applicability. If the molecules or Kondo clouds are too long in size, eventually not even DMRG can handle the very long chains needed for a proper description. For completeness, and to assure a balanced description of the technique, one of these difficult cases is also presented in our paper. But often the qualitative physics can be understood by relaxing parameters; thus, we expect that even in very complicated cases the proposed technique will be helpful, at least

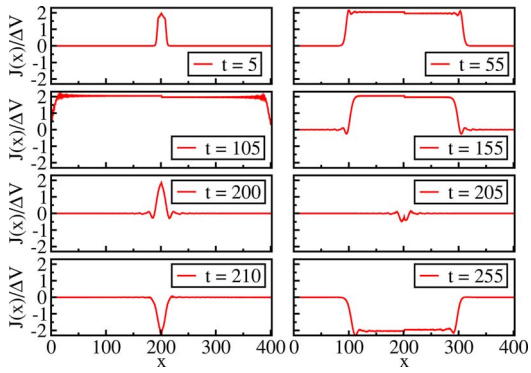

FIG. 3. (Color online) This figure shows the propagation of the current in the cluster after the bias $\Delta V=0.001$ is applied at $t=0$. The different panels show the current as a function of position x along the chain, at different times t. The size is $L=402$ and the dot is at the site 201. The results were obtained exactly, since the Hubbard couplings are zero.

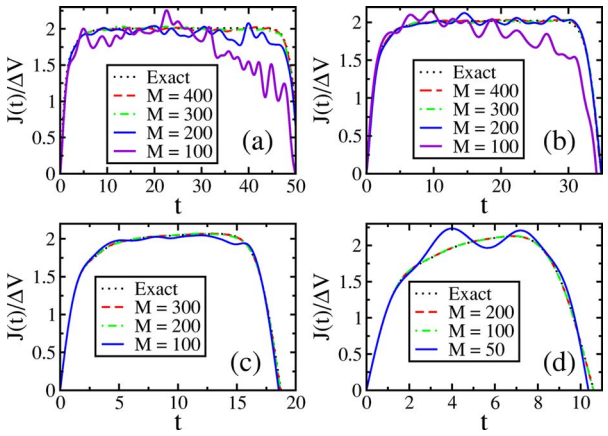

FIG. 4. (Color online) DMRG results compared to the exact results for $J(t)/\Delta V$ obtained using different clusters L and number of states M, with $\Delta V=0.001$. (a) $L=96$, (b) $L=64$, (c) $L=32$, and (d) $L=16$. Note that for $L=96$ and 64, $M=200$ shows good qualitative agreement and $M\geqslant 300$ even shows good quantitative agreement with the exact results. For $L=32$ and 16, $M=200$ and 100 already show excellent quantitative agreement with the exact results.

at the conceptual level. Other limitations of the present technique is that energy dissipation is not incorporated, and the temperature is restricted to be zero. Improving on these issues is a task left for the near future.

It is important to remark that there are other numerical techniques that can also be used to study transport in strongly correlated nanosystems. One of them is the numerical renormalization group (NRG), which evolved from Wilson's original RG ideas. This technique is quite accurate, as exemplified by some recent calculations,[26] but it cannot be used for arbitrary problems. Since our goal is to try to develop a method that can handle the fairly complex models that will be used in the near future to represent, e.g., small molecular conductors, this method does not have sufficient flexibility for our purposes. In cases where NRG works, it should be the method of choice, but this occurs in a small subset of problems in the area of transport across correlated systems. A second approach relies on the static DMRG method, using a ring geometry and with a current induced by a flux threading the ring.[27] A recently proposed third method combines linear response Kubo theory with static DMRG, and the conductance is calculated based on correlation functions in the ground state.[29] A fourth method relies on the Quantum Monte Carlo technique to calculate Green functions and the conductance of impurity models.[30] It would be interesting to find out if the methods of Refs. 27, 29, and 30 can reach a similar accuracy as ours for the case of the one and two quantum dots. A fifth method is the exact diagonalization (ED) technique followed by a Dyson equation embedding (DE) procedure (ED+DE),[31,32] where the interacting region is solved exactly (including some sites of the leads), and then the rest of the leads are taken into account via a Dyson self-consistent approach. The method directly treats bulk systems, contrary to the DMRG technique (which is necessarily limited to a large but finite chain), it is flexible, and has led to interesting results for difficult cases, such as center-of-mass phonons in molecular conductors, and multilevel systems.[33–37] However, the Dyson embedding is somewhat arbitrary and it is difficult to control its accuracy. It is our intention in the near future to combine the ED+DE method with the DMRG approach discussed in this paper, and for the physical problems where these independent techniques give similar results, then the case can be made that a reliable conclusion has been reached. Thus,ED+DE and the present method are complementary.

The organization of this paper is as follows. After the present introduction, in Sec. II, the models are defined and the technique is very briefly described. Section III contains the important test of noninteracting electrons (note that although the Coulombic coupling is zero, there are different hopping amplitudes at different links). Here, the systematic behavior of the method is discussed in detail. Section IV deals with the case of a quantum dot, with a nonzero Hubbard coupling. The value of U is comparable to the hoppings to prevent the Kondo cloud from reaching huge sizes that would render the DMRG method useless (nevertheless, one "large" U case is studied for completeness to illustrate the limitations of the method). Section V contains the case of two dots, which themselves can be coupled into a "singlet" preventing conduction or loosely coupled having individually a Kondo effect. The conclusions in Sec. VI briefly summarize our findings.

II. MODEL AND CONDUCTANCE CALCULATION

In general, the systems studied here consist of a relatively small region where Coulomb interactions are present, weakly coupled to two noninteracting leads (see Fig. 1). The interacting region can represent one or several quantum dots (QDs), a single-molecule conductor, or other nanoscopic regions. In fact, the generality of the method presented in this paper allows for a wide variety of interacting systems.

The leads are modeled as ideal tight-binding chains. As examples, the focus will be on one QD and two QDs connected in series. The total Hamiltonian of theses systems can be written in general as

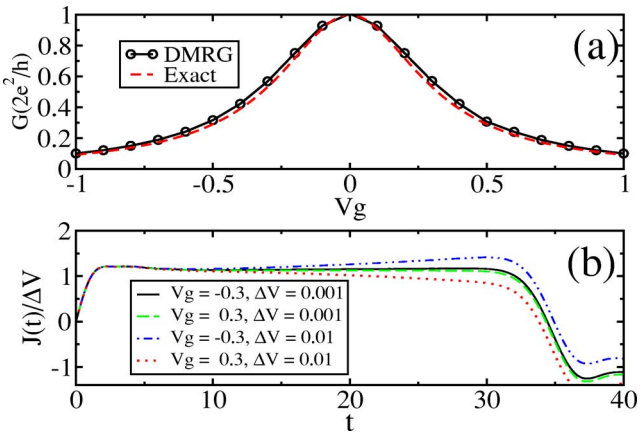

FIG. 5. (Color online) (a) DMRG and exact results for G vs V_g in the case of one noninteracting QD, and $t'=0.4$ (with $\Delta V=0.001$). The DMRG results are obtained with $L=64$ and $M=300$. In this case, G is obtained from the value of the steady-state current plateau. The exact results are for infinite leads. The results show a resonant tunneling peak of full width at half maximum (FWHM) equals $4t'^2$ at $V_g=0$. (b) $J(t)/\Delta V$ for $V_g=\pm 0.3$ and $\Delta V=0.01$, 0.001. Note that decreasing the bias voltage reduces the asymmetry between positive and negative V_g and gives a better steady-state plateau.

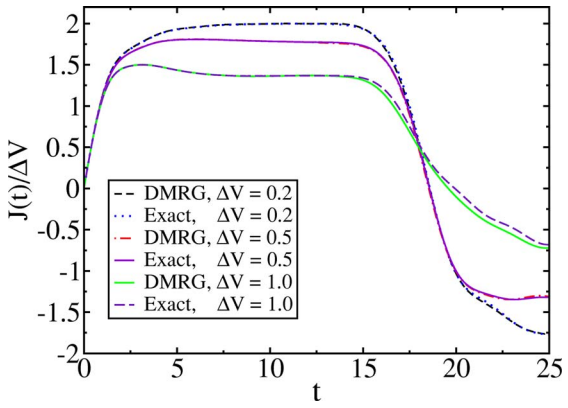

FIG. 6. (Color online) (a) DMRG results compared to the exact results in the case of one noninteracting QD for several intermediate and large values of ΔV, namely, exploring the influence of a finite bias in the calculations. The parameters used are $V_g=U=0$, and $t'=0.4$. Both DMRG and exact results are obtained with a cluster $L=32$, using $M=200$ states, for the DMRG results.

$$\hat{H}=\hat{H}_{\text{leads}}+\hat{H}_{\text{cluster}}+\hat{H}_{\text{cluster-leads}}, \tag{1}$$

where $\hat{H}_{\text{leads}}$ is the Hamiltonian of the leads, which is

$$\hat{H}_{\text{leads}}=-t_{\text{leads}}\sum_{i\sigma}[c^{\dagger}_{li\sigma}c_{li+1\sigma}+c^{\dagger}_{ri\sigma}c_{ri+1\sigma}+\text{H.c.}]. \tag{2}$$

t_{leads} is the hopping amplitude in the leads, which in the following is taken as the energy scale (i.e., $t_{\text{leads}}=1$). The operator $c^{\dagger}_{li\sigma}$ ($c^{\dagger}_{ri\sigma}$) creates an electron with spin σ at site i in the left (right) lead. $\hat{H}_{\text{cluster}}$ is the Hamiltonian of the cluster where the interactions are present. Finally, $\hat{H}_{\text{cluster-leads}}$ is the Hamiltonian that connects the interacting region to the leads, typically a hopping term. In all the results presented below, the half-filling case $n=1$ was considered in the entire system.

A. One quantum dot

For the case of one QD, represented simply by one active level, $\hat{H}_{\text{cluster}}$ can be written as

$$\hat{H}_{\text{cluster}}=V_g n_d+Un_{d\uparrow}n_{d\downarrow}, \tag{3}$$

where the first term represents the location of the energy level of the QD controlled by the gate voltage V_g. The second term represents the Hubbard repulsion between electrons of opposite spins occupying the QD. $n_d=n_{d\uparrow}+n_{d\downarrow}$ is the number of electrons at the dot. $\hat{H}_{\text{cluster-leads}}$ can be written as

$$\hat{H}_{\text{cluster-leads}}=-t'\sum_{\sigma}[c^{\dagger}_{l\sigma}c_{d\sigma}+c^{\dagger}_{r\sigma}c_{d\sigma}+h.c.], \tag{4}$$

where t' is the amplitude for the electronic hopping between the QD and the leads. $c^{\dagger}_{d\sigma}$ creates and electron with spin σ at the dot, while $c^{\dagger}_{l\sigma}$ creates an electron at the last site of the left lead and $c^{\dagger}_{r\sigma}$ creates an electron at the first site of the right lead, if sites are numbered from left to right.

B. Two coupled quantum dots in series

In the case of two QDs, $\hat{H}_{\text{cluster}}$ can be written as

$$\hat{H}_{\text{cluster}}=\sum_{\alpha=1,2}[V_g n_{d\alpha}+Un_{d\alpha\uparrow}n_{d\alpha\downarrow}]-t''\sum_{\sigma}[c^{\dagger}_{d1\sigma}c_{d2\sigma}+\text{H.c.}], \tag{5}$$

where $n_{d\alpha}=n_{d\alpha\uparrow}+n_{d\alpha\downarrow}$ is the number of electrons at the quantum dot α, and t'' is the hopping between the two dots. $\hat{H}_{\text{cluster-leads}}$ is written as

$$\hat{H}_{\text{cluster-leads}}=-t'\sum_{\sigma}[c^{\dagger}_{l\sigma}c_{d1\sigma}+c^{\dagger}_{r\sigma}c_{d2\sigma}+\text{H.c.}]. \tag{6}$$

C. Conductance calculation

The current at any time t between nearest-neighbor sites i and j is calculated as

$$J_{ij}(t)=i\frac{2\pi e}{h}t_{ij}\sum_{\sigma}\langle\Psi(t)|(c^{\dagger}_{i\sigma}c_{j\sigma}-c^{\dagger}_{j\sigma}c_{i\sigma})|\Psi(t)\rangle, \tag{7}$$

where $|\Psi(t)\rangle$ is the wave function of the system at time t, which will be calculated with the DMRG method, using a number M of states in the process. $c^{\dagger}_{i\sigma}$ creates an electron with spin σ at site i, which can be part of the interacting region or be at the leads. In the results presented below, the current shown without any link or site index corresponds to

$$J(t)=(J_L(t)+J_R(t))/2, \tag{8}$$

where $J_L(t)$ is the current between the last site of the left lead and the first dot, and $J_R(t)$ is the current between the last dot and the first site of the right lead, moving from left to right. The conductance G can be obtained by simply dividing the

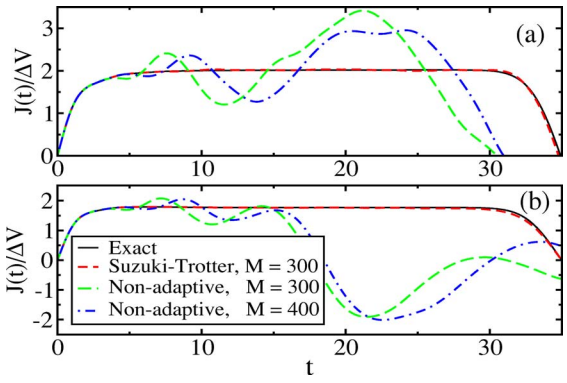

FIG. 7. (Color online) The results obtained with the Suzuki-Trotter approach and the static Runge-Kutta method compared to the exact results for (a) $\Delta V=0.001$ and (b) $\Delta V=0.5$. The parameters used are $V_g=U=0.0$, $t'=0.4$, and $L=64$.

steady-state current by the total bias ΔV. The individual voltages $\pm\Delta V/2$ in the leads are applied uniformly in each one, as indicated in Fig. 1. Note that the use of a symmetrized current $J(t)$ is convenient to obtain smoother results, particularly when the left and right leads have a different number of sites.

D. Technique

Closely following Ref. 21, a brief description of the numerical technique is here provided for completeness. The basic idea is to incorporate the Suzuki-Trotter (ST) decomposition of the time-evolution operator[23] into the DMRG finite-system algorithm.[21,22] The second order ST decomposition of the one-dimensional (1D) Hamiltonian as employed in Ref. 21 can be written as

$$e^{-i\tau H} \approx e^{-i\tau H_1/2} e^{-i\tau H_2/2} \cdots e^{-i\tau H_2/2} e^{-i\tau H_1/2}, \tag{9}$$

where H_j is the Hamiltonian of the link j. The DMRG representation of the wave function at a particular step j during the finite-system sweep is

$$|\psi\rangle = \sum_{l\alpha_j\alpha_{j+1}r} \psi_{l\alpha_j\alpha_{j+1}r} |l\rangle|\alpha_j\rangle|\alpha_{j+1}\rangle|r\rangle, \tag{10}$$

where l and r represent the states of the left and right blocks (in a truncated basis, optimally selected as eigenvectors of a density matrix), while α_j and α_{j+1} represent the states of the two central sites. An operator A acting on sites j and $j+1$ (namely, only involving nearest neighbors) can be applied to $|\psi\rangle$ exactly, and reexpressed in the same optimal basis as

$$[A\psi]_{l\alpha_j\alpha_{j+1}r} = \sum_{\alpha'_j\alpha'_{j+1}} A_{\alpha_j\alpha_{j+1};\alpha'_j\alpha'_{j+1}} \psi_{l\alpha'_j\alpha'_{j+1}r}. \tag{11}$$

Thus, the time evolution operator of the link j can be applied exactly on the DMRG step j. As a consequence, the time evolution is done by applying $e^{-i\tau H_1/2}$ at DMRG step 1, $e^{-i\tau H_2/2}$ at DMRG step 2, and so on, thus forming the usual left-to-right sweep. Then, applying all the reverse terms in the right-to-left sweep. A full sweep evolves the system one time step τ. The error introduced by the second-order decomposition is order τ^3 in each time step.[21] Thus, upon evolving the system one time unit ($1/\tau$ steps), an order τ^2 error is introduced. Numerically, the influence of this small systematic error is easy to control. In all the presented results, a time step $\tau=0.05$ was used. Note that the Trotter decomposition error is dominant at short times, whereas at longer times, the DMRG truncation error dominates. Decreasing τ would decrease the Trotter error. However, in the case of a very small τ, more DMRG sweeps are required to evolve the system one time unit thus accumulating the DMRG truncation errors. Therefore, for a given system, an optimal τ should be found. (See Ref. 24 for an analysis of this error). This brief summary gives the reader a rough idea of the technique used here. Details regarding lattice sizes, number of states kept in the DMRG procedure,and influence of other parameters are discussed below.

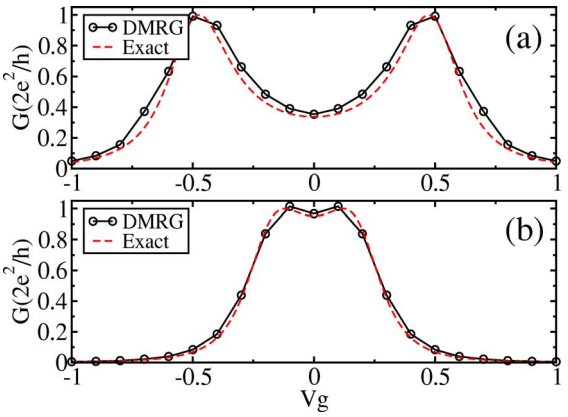

FIG. 8. (Color online) DMRG and exact results for G vs V_g in the case of two coupled noninteracting QDs. The DMRG results are obtained with $L=64$ and $M=300$ ($\Delta V=0.001$). The exact results are for infinite leads. The cases (a) $t''=0.5$ and (b) $t''=0.2$ are investigated, with $t'=0.4$ in both cases. The results present the bonding and anti-bonding resonant tunneling peaks at $\pm t''$.

III. NONINTERACTING CASE

Properties of the method discussed in this paper are exemplified in Fig. 2(a), where the current at the center of the chain is shown (divided by the voltage difference) as a function of time. The current in this figure is *exactly* calculated, not using DMRG, since for noninteracting particles the problem reduces to a single electron problem. A small bias $\Delta V=0.001$ will be used, unless otherwise stated. Thus, in this first study the focus will be on trying to reproduce results expected from linear response, but a few results with a finite bias are also included in this paper, as discussed below. Returning to Fig. 2(a), for a bulk system the current would be expected to raise for a small fraction of time, and then reach a steady state. This indeed occurs even in our finite-size systems. In fact, the transition from zero current at $t=0$ to an approximately time-independent current regime is very fast and can be barely observed in the scale of Fig. 2(a). But the existence of a very flat plateau in the current is clear, and its value will be used to extract the conductance below. Note that due to the finite size of the system, the current cannot

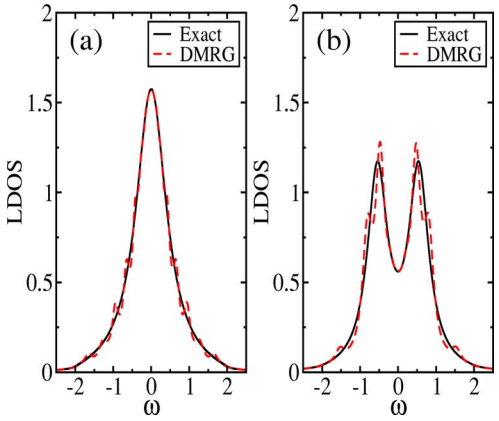

FIG. 9. (Color online) DMRG local density-of-states (LDOS) results for (a) 1QD and (b) 2QDs compared to the exact (bulk) results. The parameters used are $V_g=U=0$, $t'=0.4$ in both cases and $t''=0.5$ in (b). In (a), a broadening imaginary component $\eta=0.1$ was introduced. In (b), $\eta=0.15$. Smaller values of η would reveal the discrete nature of the LDOS obtained with DMRG on a finite $L=64$ system.

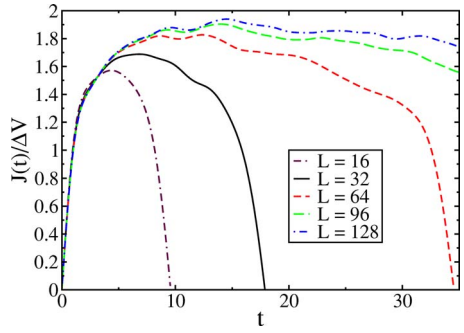

FIG. 10. (Color online) $J(t)/\Delta V$ in the case of one quantum dot for different cluster lengths L. The parameters used are $U=1.0$, $t'=0.4$, $\Delta V=0.005$, and $V_g=-0.5$. As L increases, the conductance approaches the unitarity limit $(2e^2/h)$ due to the Kondo screening effect.

continue in the same steady state at all times. The Hamiltonian is particle number conserving, and as a consequence, the presence of a current implies a population-depopulation of the leads, which cannot continue forever. In fact, once the front of the charge pulse reaches the end of the chain, it bounces back and eventually generates a current of the opposite sign. This effect will be discussed in more detail later. Here, it is important to remark that in spite of this periodicity present in finite open-end systems, the flat plateaus are clearly defined over an extended period of time for the lattice of 402 sites used, and the value of the conductance can be easily deduced from those individual plateaus, as discussed below. Note that the setup of Fig. 1 and the existence of plateaus in the current Fig. 2 are natural in the DMRG-transport context and was observed before.[38] Our main contribution will be the use of the adaptive DMRG method for the calculations, as shown below.

To further illustrate the propagation of charge in the cluster after the finite bias is switched on at time $t=0$, in Fig. 3 the exact current at different positions x is shown, parametric with time. At small times, $t=5$ (in units of $\hbar/t_{\text{leads}}$), only the central portion is affected as expected. At time $t=55$, the affected region is much larger, whereas at $t=105$, the front has reached the ends of the chain and soon after it starts bouncing back. At times $t=200$ and 205, approximately, the initial condition is recovered, and almost everywhere the current to the left and right cancel out nearly exactly. For larger times, a reverse sign current is created. Note that in our studies there are *no* sources of dissipation, and the current will keep on oscillating forever. Adding inelastic processes is a next major challenge in this context, left for the future.

It is also important to show that the existence of the plateaus is not restricted to very long chains of hundreds of sites, but they are visible on much smaller systems, increasing the chances that the numerical DMRG method can be used even for complicated nanosystems. Figure 2(b) contains the current vs time for a variety of lattice sizes, ranging from 402 to systems as small as 16 sites. The time width of the plateaus depends on L, as expected, but the value of the current at the plateaus is approximately L independent even up to systems as small as containing $L=32$ sites. Even the $L=16$ chain has a periodicity with a first plateau in the current, which is also in good agreement with the expected value from larger sizes. Thus, this behavior appears to be robust and the plateaus are also expected to be present for the chains that the DMRG method can handle. That this is the case can be shown in Fig. 4, where DMRG results for the current vs time are shown, compared to exact data. Consider first a sufficiently long chain, as shown in Fig. 4(a), such that a sharp plateau is observed in the exact result. Figure 4(a) shows that increasing the number of states M used in the DMRG approximation, a convergence to the exact solution is observed. In fact, for $M=300$ or higher, the DMRG results cannot be distinguished from the exact ones. A similar behavior is found using shorter chains as for the case with $L=64$ sites Fig. 4(b); but in this example, the plateau can be observed accurately even with a smaller number of states such as $M=200$. The trend continues for smaller systems Figs. 4(c) and 4(d): For $L=32$ and 16, the DMRG method reproduces the exact results with high accuracy using ~ 100 states.

Figure 5(a) shows the conductance deduced from the behavior of the current obtained with the DMRG method vs the gate voltage V_g, for the case of a single "noninteracting" quantum dot, namely, one having $U=0$. The hopping amplitude between the dot and the leads is $t'=0.4$. It is expected that the maximum value of the conductance be obtained when the level in the dot is aligned with the Fermi level of the leads, and this occurs in our case at $V_g=0$. The DMRG results beautifully confirm this expectation. As the gate voltage changes away from 0, the conductance is expected to decrease symmetrically and this is indeed shown in Fig. 5(a). In fact, the results at nonzero gate voltage are also in excellent quantitative agreement with the exact results.

All the previous results were obtained for a sufficiently small value of the bias voltage $\Delta V=0.001$, as already explained. It is interesting to observe how the results change when larger values of ΔV are employed. Figure 5(b) shows the current for a couple of biases. The existence of the pla-

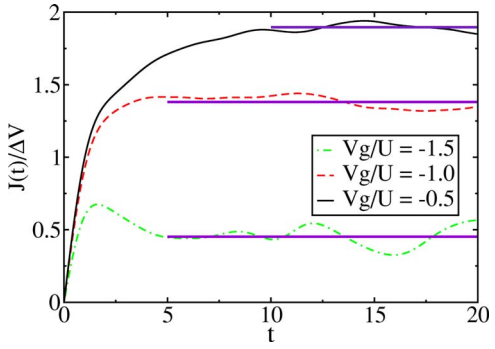

FIG. 11. (Color online) $J(t)/\Delta V$ in the case of one interacting QD for different values of V_g, and with $\Delta V=0.005$. The value of the conductance is obtained by averaging the current over an interval of time, corresponding to the steady state. The solid horizontal lines represent this time interval over which the average of the current is taken, and the value of the average. The parameters used are $U=1.0$, $t'=0.4$, $L=128$, and $M=300$.

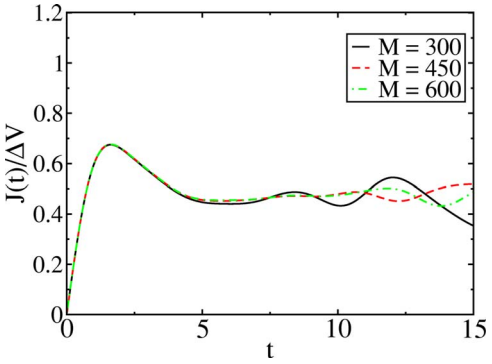

FIG. 12. (Color online) $J(t)/\Delta V$ in the case of one interacting QD for $V_g/U=-1.5$, $U=1.0$, $t'=0.4$, $L=128$, and different values of M. Note that as M increases, the oscillations at long times tend to decrease.

teau is clear in both cases, but for $\Delta V=0.01$, asymmetries between positive and negative gate voltages can be observed, which are not expected in the limit $\Delta V\to 0$. As a consequence, the rest of the results discussed below were obtained with $\Delta V=0.001-0.005$ unless otherwise noted. An easy criterion to realize if a sufficiently small bias is used to obtain the linear response limit is to repeat the calculations for the same amplitude of gate voltage, but opposite signs, and see if a noticeable difference is obtained.

The method proposed here also works in the case of a finite bias voltage, namely, it is not restricted to the linear response regime. To show that the technique can handle even a large bias, in Fig. 6 results for the current vs. time are shown at the indicated voltages. It is only at ΔV as large as 1.0 that small differences are visually observed in the figure, between the DMRG and exact results. This can be easily fixed increasing the number of states M. Thus, overall the method appears to be sufficiently robust to handle arbitrary voltages, showing the generality of the technique here proposed. Nevertheless, further work in the finite bias context will be important to fully test this case, calculating differential conductances and analyzing the regime of very strong bias.

In our investigations, the numerical study was also carried out using a "static" procedure, where the $t=0$ DMRG basis is not expanded with growing time. In this case, the results are obtained by integrating the time-dependent Schrödinger equation using the fourth-order Runge-Kutta method, and also using the DMRG ground state as the initial state.[17] This is to be contrasted with the procedure of Refs. 21 and 22, where the basis is modified with time. Figure 7 shows the results of both procedures: Clearly using an adaptive basis provides superior data, reproducing accurately the exact results. In the static procedure a similar accuracy is reached only by increasing substantially the number of states, thus missing its economical CPU-time advantages.

The method discussed here also works nicely for the case of two noninteracting QDs, as shown in Fig. 8 for two different values of the hopping amplitude t'' between the dots. The slight difference between the DMRG and the bulk exact results can be improved increasing the number of sites.

Although not directly related to the method to obtain the conductance of an interacting nanosystem discussed in this paper, for completeness we have also studied the local density-of-states which are important to guide the intuition and contrast with other methods and scanning tunneling microscopy experiments as well. The local density-of-states at the dot is given by $\rho_d(\omega)=\Sigma_\sigma\rho_{d\sigma}(\omega)=-\frac{1}{\pi}Im[\Sigma_\sigma G^R_{d\sigma}(\omega)]$, where $G^R_{d\sigma}(\omega)$ (the retarded Green's function) can be written as

$$G^R_{d\sigma}(\omega)=\left\langle\Psi_0|c_{d\sigma}\frac{1}{\omega+E_0-\hat{H}+i\epsilon}c^\dagger_{d\sigma}|\Psi_0\right\rangle+\left\langle\Psi_0|c^\dagger_{d\sigma}\frac{1}{\omega-E_0+\hat{H}+i\epsilon}c_{d\sigma}|\Psi_0\right\rangle$$

In the results shown, $G^R_{d\sigma}(\omega)$ is evaluated using the continuous fraction expansion technique with coefficients calculated with the DMRG method.[14] In Fig. 9, results for noninteracting quantum dots are shown (namely, dots where the Hubbard repulsion is 0). Clearly, both the exact results (which are shown already in the bulk limit) and the DMRG results, slightly smeared by shifting, using a small imaginary component η, the pole locations in the continued fraction expansion, are in excellent agreement in both cases. A smaller η would have revealed the many δ functions in the DMRG case obtained using a finite chain with 64 sites.

IV. ONE QUANTUM DOT

In the previous sections, the method was introduced and tested for the case of noninteracting $U=0$ electrons. But the main application of the technique is envisioned to occur in the presence of nontrivial Coulombic interactions (and eventually also adding phononic degrees of freedom). In this section, the case of a nonzero Hubbard coupling will be considered, focusing on the special case of one quantum dot. The Hamiltonian used was already discussed in previous sections.

A. Results at intermediate values of U

Figure 10 contains our DMRG results for the current vs time, for the case of $U=1.0$. Similar values of this coupling were extensively used in previous investigations,[31,33–37] and

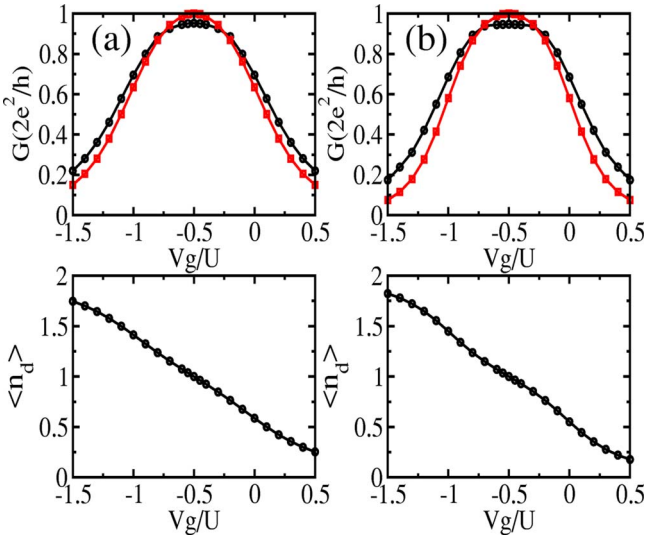

FIG. 13. (Color online) Conductance G and the dot occupation $\langle n_d \rangle$ for one interacting QD. The circles show G obtained by averaging the current over an interval of time corresponding to the steady state, as shown in Fig. 11. The squares show G obtained from $\langle n_d \rangle$ using the Friedel sum rule (FSR). G has the shape of the expected Kondo or mixed-valence plateau centered at $V_g = -U/2$. The feature would be sharper reducing t'. Results shown are: (a) $U=1.0$, $t'=0.4$, and (b) $U=2.0$, $t'=0.5$. In both cases, $L=128$ and $M=300$. Note that the DMRG conductance results in (a) show a slightly better agreement with the FSR results. This is expected since the finite-size effects are stronger for larger U.

it is believed to lead to a Kondo cloud of a size amenable to numerical investigations (note that if U is very large, the effective J between localized and mobile spins is reduced, and it is known that the cloud's size rapidly grows with decreasing J). The figure shows that the systematic behavior found in the noninteracting case survives the presence of a Coulomb interaction; namely, the current develops plateaus that can be used to determine the conductance. For instance, this effect is clearly present for $L=96$ and 128, although for smaller sizes (shown for completeness) the maximum current is 10–20% less than expected and one must be cautious with size effects. The value of the gate voltage is $-U/2$, which in the absence of the Kondo effect would locate the system in the conductance "valley" (implying a near-zero conductance) between the Coulomb blockade peaks at $-U$ and 0. The figure shows that the method introduced in this paper is able to reproduce the existence of a Kondo effect, since the conductance is actually very close to the ideal limit $2e^2/h$,[9,31,33,34] rather than being negligible. This is a highly nontrivial test that the proposed technique has passed.

Results for other values of the gate voltage are shown in Fig. 11. Moving away from $V_g=-U/2$, the current is reduced, as discussed below in more detail. Note that the plateaus contain small oscillations as a function of time.[39] The size of the oscillations give an indication of the errors in the numerical determination of the conductance, for a given lattice size. The procedure followed here to extract the current needed for the calculation of the conductance is to carry out averages over time, as shown in Fig. 11, in the plateau region between the short-time intrinsic oscillations and the long-time oscillations caused by numerical errors. For a given L, as M increases, the oscillations tend to disappear. This is shown in Fig. 12.

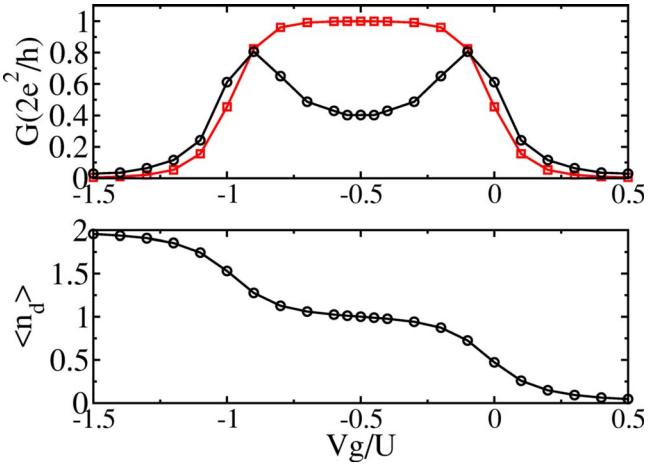

FIG. 14. (Color online) Conductance $G(\Delta V=0.001)$ and charge at the dot $\langle n_d \rangle$, for one interacting QD in the case of large U. The circles show G obtained from DMRG current procedure outlined in this paper, while the squares show G obtained from $\langle n_d \rangle$ using the Friedel sum-rule. The finite-size effects are obvious here, since the results are halfway between the expected Kondo plateau (properly reproduced by the FSR procedure) and the Coulomb blockade peaks. This case is shown as an illustration of important size effects in some limits. The parameters used are $U=4.0$, $t'=0.4$, $L=128$, and $M=300$.

Following the procedure sketched in Fig. 11, the full conductance vs V_g was prepared for U equal to 1 and 2. The results are in Fig. 13. The results are compared to the conductance obtained using the Friedel sum rule (FSR), $G = \frac{2e^2}{h} \sin^2\left(\frac{\pi}{2}\langle n_d \rangle\right)$. The shape of the curve is the expected one for the regime considered here: the intermediate values of U do not locate our investigation deep in the Kondo regime, with sharply defined integer charge at the dot, but more into the mixed-valence region. This can be deduced from the value of the dot charge vs V_g, also shown in Fig. 13. With increasing U and/or decreasing t', sharper charge steps are formed, but the Kondo cloud size increases, as discussed later.

B. Results at large values of U

There are cases where the technique gives results that are only qualitatively correct. Although, clearly, further increases of the number of states and lattice sizes will improve the accuracy, it is important to judge if at least the essence of the physics has been captured by our proposed method. In Fig. 14, results for $U=4$ are shown. This is a representative of the "large" U regime, since it must be compared to t' (as opposed to $t_{\text{leads}}=1$) that is only 0.4 in this figure. Another indication that this U is large is in Fig. 14(b), where a clear sharp quantization of the charge inside the dot is observed. In this large-U regime, the DMRG conductance is shown in Fig. 14(a). Clearly, there is a substantial difference between the Friedel sum-rule estimation (which has the correct "box"

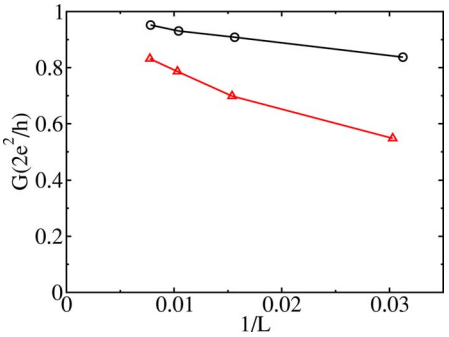

FIG. 15. (Color online) Finite-size scaling of the conductance G at $V_g=-U/2$ for the odd-1QD-even (circles) and even-1QD-even clusters (triangles) setups. Note that in both cases G converges to 1 in the bulk limit. However, the odd-1QD-even cluster converges faster, which makes it the most useful for practical calculations. The parameters used are $U=1.0$ and $t'=0.4$.

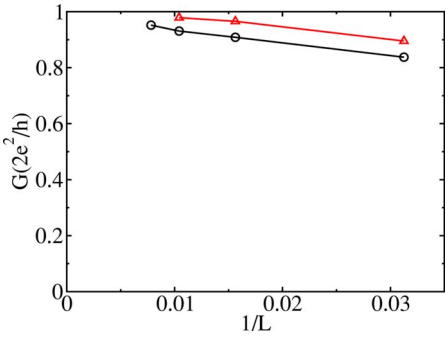

FIG. 16. (Color online) Finite-size scaling of G for odd-QD-even clusters using OBC (circles) and DBC (triangles). $d=0.5$ was used. Note that $L=64$ cluster with DBC gives better results than a $L=128$ cluster with OBC. The same parameters are used as in Fig. 15.

shape in the gate voltage range $[-U,0]$) and the DMRG numbers. However, at least the fact that there must be a nonzero conductance at $V_g=-U/2$ was properly captured by the method. This example illustrates a case where size effects are important, due to the subtle rapid increase of the Kondo cloud with increasing U. The results in this case show a slow convergence with L toward the FSR results. However, the qualitative results were captured, in spite of the fact that to reach a quantitative conclusion much larger sizes must be considered, or a careful finite-size scaling should be done. This case is shown as a cautionary example to the readers, who must be alert of the limitations of the numerical methods. Note that while FSR results are excellent, for other arbitrary cases it would be unclear whether the Friedel sum-rule method is valid and, as a consequence, not always this procedure can be used.

C. Improving the convergence

To carry out the investigations presented thus far in this and the previous section, the number of sites in the leads at left and right of the dot region have been chosen such that one lead has an *even* number and the other an *odd* number of sites (to refer to this case, the notation used below will be "odd-QDs-even"). Although this should be irrelevant for very long chains, in practice this is important for the speed of convergence of the conductance calculations with increasing cluster size. For example, in the interacting case $U\neq 0$, a Kondo or mixed-valence regime is expected where the spin at the dot couples with electrons at the Fermi level of the leads. This formation of the Kondo cloud occurs more efficiently on a finite-size lattice if already a zero energy level is available, as it occurs when one of the leads has an odd number of sites. That this improves the rate of convergence with increasing lattice size is shown in Fig. 15, where the odd-1QD-even case is contrasted to the even-1QD-even case, where in both leads the number of sites is even. Clearly, the odd-1QD-even case approaches the ideal limit $2e^2/h$ faster than using leads with an even number of sites, and it is recommended to be used in future investigations. Figure 15 also shows that, eventually, with sufficiently large systems, both combinations will reach the same ideal result, as expected. The remaining possibility (odd-1QD-odd) was also investigated (not shown). For reasons that remain to be analyzed further, the convergence in this case is not as good as in the odd-1QD-even case. As a consequence, empirically it is clear that the combination even-QDs-odd is the most optimal to speed up the size convergence of the calculation.

Another method to improve the size convergence was tested. Following Refs. 28 and 29, the finite-size effects can be reduced by using "damped boundary conditions" (DBC). The hoppings in the M_D links at the boundaries are reduced using the formulas $-td,-td^2,\ldots,-td^{M_D}$, where $d<1$. M_D has to be chosen such that the damping occurs far enough from the central region. Figure 16 shows the finite-size scaling using odd-QD-even clusters and the same parameters as in Fig. 15, both with DBC and the standard open boundary conditions (OBC) used in the rest of the paper. The latter indeed improves the convergence. Although in the present study, OBC were used in most of the paper to keep the simplicity in the presentation and reduce the number of parameters, the use of DBC is recommended for cases where size effects are strong.

D. Influence of magnetic fields

To fully confirm that our investigations in the Kondo–mixed-valence regime have captured the essence of the problem, namely the formation of a Kondo cloud with antiferromagnetic coupling between the spins at the leads and the dot, investigations including magnetic fields are necessary. In Fig. 17, it is shown how the Kondo plateau in the conductance evolves with increasing magnetic field. As expected from previous investigations, including results obtained using very different techniques, such as the Lanczos method followed by a Dyson-equation embedding procedure (ED +DE),[32] the conductance broad peak splits with increasing magnetic field B. At large B, two peaks are observed at $-U$ and 0, as it occurs also in the high-temperature regime where only Coulomb blockade effects are present.

V. TWO COUPLED QUANTUM DOTS

The method discussed in this paper is general, and, in principle, it can be implemented for a variety of complicated

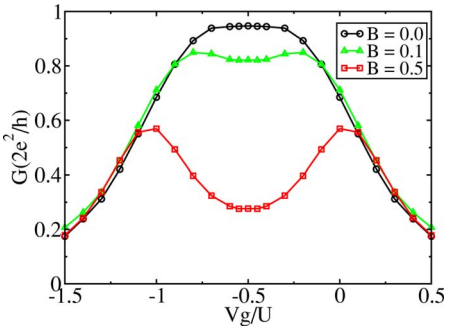

FIG. 17. (Color online) Conductance G vs gate voltage V_g in the case of one interacting QD ($U=2.0$, $t'=0.5$) for different values of the magnetic field B (and $\Delta V=0.001$). For $B=0$, a Kondo plateau is obtained, centered at $V_g=-U/2$. As B increases, the Kondo effect is suppressed, and for moderate B, two Coulomb blockade peaks are observed at $V_g=-U$ and $V_g=0$, as expected.

geometries and couplings in the interactive region between the leads. Thus, it is important to confirm that the method will keep its validity going beyond the one quantum-dot case. In this section, the case of two dots will be studied. Systems with two quantum dots are believed to be understood theoretically, and as a consequence, our numerical data can be contrasted against robust results in the literature. Cases involving more dots[33] are still not fully understood, and their analysis will be postponed for future investigations. In Fig. 18, the current vs time is shown for two dots. The Hamiltonian for this case was already defined in previous sections. For a fixed t', increasing the amplitude of the direct hopping between the dots t'' amounts to isolating the two dots system from the rest. As a consequence, the current is expected to decrease, and the method indeed reproduces this effect, as shown in Fig. 18. The same physics is obtained reducing t', at fixed t''. In fact, previous studies[40] have shown that the conductance only depends on t''/t'^2, and this has been verified using our method.

The conductance of a system with two dots in series will decrease with increasing t''/t'^2 (at large t''/t'^2) due to the decoupling of the two-dots system into a small two-sites

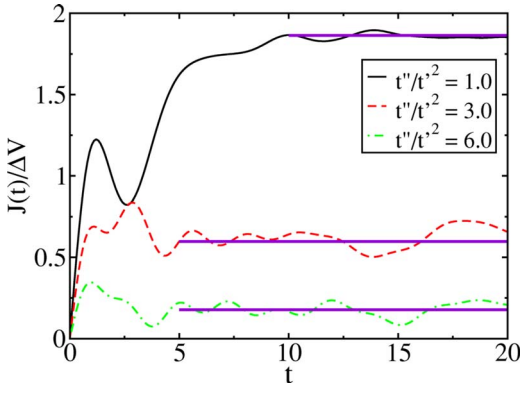

FIG. 18. (Color online) $J(t)/\Delta V$ for two coupled QD's at $V_g=-U/2$ for different values of t''/t'^2 (and $\Delta V=0.005$). As in the case of one interacting QD, the conductance is obtained by averaging the steady-state current over the indicated intervals. The parameters used are $U=1.0$, $t'=0.5$, $L=127$, and $M=300$.

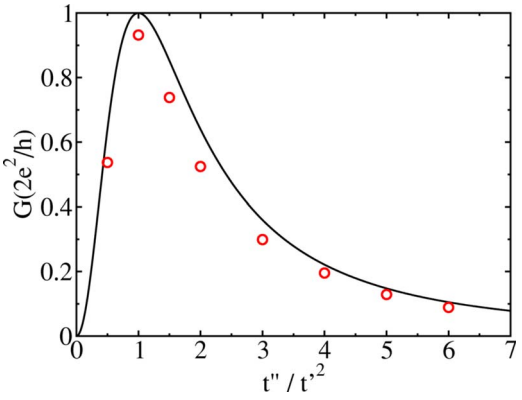

FIG. 19. (Color online) Conductance G as a function of t''/t'^2, at $V_g=-U/2$ ($\Delta V=0.005$). In this regime, G is determined by the competition between the Kondo correlation of each dot with the neighboring leads and the antiferromagnetic correlation between the two dots. The circles represent our DMRG results obtained with $L=127$ and $M=300$. The solid line is the plot of the functional form obtained by Georges and Meir using SBMFT.[40]

molecule, as already discussed. But this conductance will also be very small at small t'' when the tunneling from one dot to the next is nearly cut off. As a consequence, the conductance vs t''/t'^2 is known to present a peak at intermediate values. In Fig. 19, the slave-boson mean-field technique (SBMFT) predictions for this case obtained in previous investigations[40] are shown together with our results. The agreement is fairly reasonable, providing further support that the method discussed here can handle systems where there are competing tendencies, beyond the one quantum-dot case.

VI. CONCLUSIONS

In this paper, a method was proposed and tested to calculate the conductance of small (nanoscale) strongly correlated systems modeled by tight-binding Hamiltonians. The approach is based on the adaptive time-dependent DMRG method, and it was shown to work properly for noninteracting systems and also in the cases of one and two quantum dots. Besides the finite-size effects, discussed in the text as well, there are no other severe limitations to handle complex interacting models with arbitrary couplings. The method is a complement to DFT calculations in the nanoscopic context. Further improvements of the technique must consider temperature and inelastic effects.

It is concluded that the semiquantitative analysis of transport in models of strongly correlated nanosystems appears under reach, and much progress is expected from the application of the technique presented here to realistic Hamiltonians for small molecules and arrays of quantum dots. The remarkable cross-fertilization between modeling, simulation, and experiments existing in bulk strongly correlated materials, such as transition-metal oxides, can be repeated in a variety of interesting systems at the nanoscale.

ACKNOWLEDGMENTS

The authors thank Brad Marston, Eduardo Mucciolo, Marcelo Rosenberg, Peter Schmitteckert, and Ulrich Schollwöck for useful comments. The work of K.A., C.B., and E.D. was partially supported by the NSF Grant No. DMR-0454504.

[1] A. Aviram and M. A. Ratner, Chem. Phys. Lett. **29**, 277 (1974). See also A. Aviram, Nature (London) **408**, 541 (2000); M. A. Ratner, Science **300**, 1384 (2003); J. R. Heath and M. A. Ratner, Phys. Today **43**, 43 (2003); and references therein.

[2] J. Chen, M. A. Reed, A. M. Rawlett, and J. M. Tour, Science **286**, 1550 (1999); W. Liang, M. P. Shores, M. Brockrath, J. R. Long, and H. Park, Nature (London) **417**, 725 (2002); and references therein.

[3] M. Kastner, Phys. Today **46**, 24 (1993); R. C. Ashoori, Nature (London) **379**, 413 (1996).

[4] Supriyo Datta, Weidong Tian, Seunghum Hong, R. Reifenberger, Jason I. Henderson, and Clifford P. Kubiak, Phys. Rev. Lett. **79**, 2530 (1997); and references therein.

[5] M. DiVentra, S. T. Pantelides, and N. D. Lang, Phys. Rev. Lett. **84**, 979 (2000); and references therein.

[6] S.-H. Ke, H. U. Baranger, and W. Yang, Phys. Rev. Lett. **91**, 116803 (2003); and references therein.

[7] B. Muralidharan, A. W. Ghosh, and S. Datta, cond-mat/0505375; and references therein.

[8] D. Goldhaber-Gordon, H. Shtrikman, D. Mahalu, D. Abusch-Magder, U. Meirav, and M. A. Kastner, Nature (London) **391**, 156 (1998).

[9] L. I. Glazman and M. E. Raikh, JETP Lett. **47**, 452 (1988); T. K. Ng and P. A. Lee, *ibid.* **61**, 1768 (1988); Y. Meir and N. S. Wingreen, Phys. Rev. Lett. **68**, 2512 (1992). For a recent review, see M. Pustilnik, cond-mat/0512671 (unpublished).

[10] E. Dagotto, T. Hotta, and A. Moreo, Phys. Rep. **344**, 1 (2001). See also E. Dagotto, New J. Phys. **7**, 67 (2005).

[11] E. Dagotto, Rev. Mod. Phys. **66**, 763 (1994).

[12] S. R. White, Phys. Rev. Lett. **69**, 2863 (1992).

[13] U. Schollwöck, Rev. Mod. Phys. **77**, 259 (2005).

[14] K. A. Hallberg, Phys. Rev. B **52**, R9827 (1995).

[15] T. D. Kühner and S. R. White, Phys. Rev. B **60**, 335 (1999).

[16] E. Jeckelmann, Phys. Rev. B **66**, 045114 (2002).

[17] M. A. Cazalilla and J. B. Marston, Phys. Rev. Lett. **88**, 256403 (2002). See also Phys. Rev. Lett. **91**, 049702 (2003).

[18] H. G. Luo, T. Xiang, and X. Q. Wang, Phys. Rev. Lett. **91**, 049701 (2003).

[19] P. Schmitteckert, Phys. Rev. B **70**, 121302(R) (2004).

[20] U. Schollwöck, cond-mat/0502470 (unpublished).

[21] S. R. White and A. E. Feiguin, Phys. Rev. Lett. **93**, 076401 (2004).

[22] A. J. Daley, C. Kollath, U. Schollwöck, and G. Vidal, J. Stat. Mech.: Theory Exp. (2004), P04005.

[23] G. Vidal, Phys. Rev. Lett. **91**, 147902 (2003).

[24] D. Gobert, C. Kollath, U. Schollwöck, and G. Schütz, Phys. Rev. E **71**, 036102 (2005).

[25] A. E. Feiguin and S. R. White, Phys. Rev. B **72**, 020404(R) (2005).

[26] For recent references see P. S. Cornaglia, H. Ness, and D. R. Grempel, Phys. Rev. Lett. **93**, 147201 (2004); F. B. Anders and A. Schiller, *ibid.* **95**, 196801 (2005).

[27] R. Molina, P. Schmitteckert, D. Weinmann, R. Jalabert, G-L. Ingold, and J-L. Pichard, Eur. Phys. J. B **39**, 107 (2004); and references therein. See also V. Meden and U. Schollwöck, Phys. Rev. B **67**, 193303 (2003); See also V. Meden and U. Schollwöck, *ibid.* **67**, 035106 (2003).

[28] M. Vekic and S. R. White, Phys. Rev. Lett. **71**, 4283 (1993).

[29] D. Bohr, P. Schmitteckert, and P. Wölfle, Europhys. Lett. **73**(2), 246 (2006).

[30] L. Arrachea and M. J. Rozenberg, Phys. Rev. B **72**, 041301(R) (2005).

[31] V. Ferrari, G. Chiappe, E. V. Anda, and M. A. Davidovich, Phys. Rev. Lett. **82**, 5088 (1999); M. A. Davidovich, E. V. Anda, C. A. Bussr, and G. Chiappe, Phys. Rev. B **65**, 233310 (2002).

[32] M. E. Torio, K. Hallberg, A. H. Ceccatto, and C. R. Proetto, Phys. Rev. B **65**, 085302 (2002).

[33] C. A. Büsser, A. Moreo, and E. Dagotto, Phys. Rev. B **70**, 035402 (2004).

[34] C. A. Büsser, G. B. Martins, K. A. Al-Hassanieh, A. Moreo, and E. Dagotto, Phys. Rev. B **70**, 245303 (2004).

[35] G. B. Martins, C. A. Büsser, K. A. Al-Hassanieh, A. Moreo, and E. Dagotto, Phys. Rev. Lett. **94**, 026804 (2005).

[36] G. B. Martins, C. A. Büsser, K. A. Al-Hassanieh, E. V. Anda, A. Moreo, and E. Dagotto, Phys. Rev. Lett. **96**, 066802 (2006)

[37] K. A. Al-Hassanieh, C. A. Büsser, G. B. Martins, and E. Dagotto, Phys. Rev. Lett. **95**, 256807 (2005).

[38] See P. Schmitteckert, Leiden Conference on Recent Progress and Prospects in Density-Matrix Renormalization, August, 2004.

[39] In some cases, the results show some oscillations at small times. This effect may be related with the oscillations described by N. S. Wingreen, A. P. Jauho, and Y. Meir, Phys. Rev. B **48**, R8487 (1993). We thank P. Schmitteckert for pointing out this reference to us. However, at large times the oscillations give an indication of the numerical errors.

[40] A. Georges and Y. Meir, Phys. Rev. Lett. **82**, 3508 (1999).